ACS OMEGA

http://pubs.acs.org/journal/acsodf

Article

Potentiometric Phosphate Ion Sensor Based on Electrochemical Modified Tungsten Electrode

Kebin Xu, Ying Li,* and Min Li

Cite This: *ACS Omega* 2021, 6, 13795−13801

Read Online

ACCESS | Metrics & More | Article Recommendations | Supporting Information

ABSTRACT: Determination of phosphate ions in aqueous solutions attracts a great deal of interest in the areas of environment, medicine, and agriculture. As phosphoric acid is a poly basic acid, the different forms of existence at different pH result in direct determination facing a big challenge. Herein, we reported a potentiometric phosphate ion sensor based on a surface-modified tungsten electrode. Pure tungsten was electrodeposited at a constant potential of 0.2 V versus Ag|AgCl in Na_2HPO_4. WO_3 and $H_3O_{40}PW_{12}{\cdot}xH_2O$ were electrodeposited on the surface of the tungsten electrode. The modified tungsten electrode was used as a working electrode in a two-electrode system to detect the concentration of phosphate ions in aqueous solutions. The detection limit of the modified tungsten electrode for phosphate ions is 10^{-6} M from pH 7 to pH 8 and 10^{-5} M from pH 9 to pH 10. It has good selectivity to other common anions. The long-term monitoring experiment showed that the potential fluctuation was less than ±3 mV in 24 h. Compared to conventional determination methods, the current phosphate ion sensor showed a close value in a real sample. The mechanism of phosphate ion response was investigated in detail. This sensor possesses advantages of simple manufacture, low cost, a wide pH range for detecting, and good selectivity.

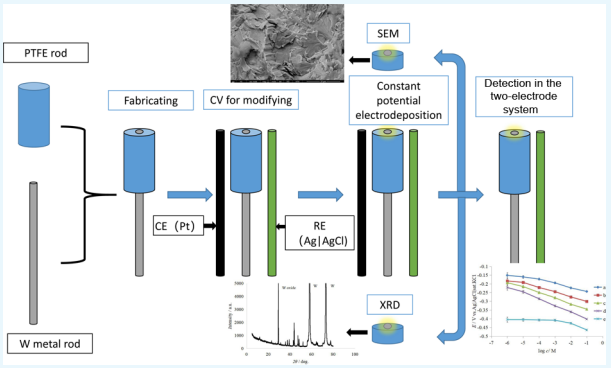

1. INTRODUCTION

Phosphate is the essential material basis for phytoplankton growth.[1−3] The bioavailability of phosphorus directly affects the global primary productivity. Phosphorus may also limit nitrogen fixation and become an important factor limiting primary productivity. The determination of phosphate content in water is also one of the important indicators of pollution investigation.[4] In recent years, the excessive discharge of phosphorus in agricultural and industrial wastewater has led to eutrophication of nearby water. As a result, algae and other planktons propagate rapidly, and the dissolved oxygen content in water decreases. Eventually, the number of algae, planktons, and aquatic organisms decreased or even disappeared.[5−7] Therefore, the accurate determination of phosphorus in water has important theoretical and practical significance for an in-depth understanding of the biogeochemical process and environmental protection.[8] Besides this, phosphorus detection is also important in the domains of medicine, pharmacology,[9−12] and agriculture.[13]

The standard method for the determination of phosphate is phosphomolybdate blue spectrometry, which is also the commonly used phosphate measurement method in the world.[14] However, the traditional spectrometer method also has some shortcomings: the operation steps are complicated, the reagent needs to be used and prepared on site, and the workload is heavy. Moreover, the turbidity in the water sample will directly affect the measured absorbance value, and there are many interference factors, so it is necessary to make compensation and correction. Therefore, the traditional spectrometer cannot meet the needs of modern environmental monitoring, such as fast, simple, and real-time online.

In recent years, the electrochemical phosphate ion sensor has been widely used in environmental analysis because of its high sensitivity and selectivity, wide linear range, fast response time, easy-to-realize online analysis and automatic control. At present, in the application of the chemical sensor technology for detecting phosphate in water, the research on liquid membrane phosphate ion-selective electrodes and solid membrane phosphate ion-selective electrodes has also made certain progress, and great progress has been made in the research and development of the phosphate anion acceptor.[15] The electrochemical phosphate ion sensor mainly includes an amperometric sensor, an impedimetric sensor, and a potentiometric sensor. Although the amperometric sensor

Received: March 8, 2021
Accepted: May 10, 2021
Published: May 20, 2021

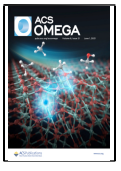

https://doi.org/10.1021/acsomega.1c00195
ACS Omega 2021, 6, 13795−13801

can usually realize a relative low detection limit, high energy consumption of the rotating electrode and applied potential increase the charge of long-tern *in situ* monitoring. Moreover, compared with the potentiometric sensor, the linear range of the amperometric sensor is commonly no more than 2 orders of magnitude.[16−18] Recently, some researchers of the impedimetric phosphate sensor reported some sensors that possess relatively good response characteristics.[19−21] However, they have a common shortcoming of complicated manufacture steps. Similar to the amperometric sensor, the impedimetric sensor also meets the problem of high electricity consumption. As for the potentiometric sensor, the phosphate ionophore was considered to be an effective tool to establish a poly(vinyl chloride)-liquid-membrane phosphate sensor.[22−25] High selectivity, a wide linear range, and a rapid response time were achieved. However, the stability and the reproducibility cannot meet the need of practical measurements to some extent. The author designed a cobalt-modified electrode as a $H_2PO_4^-$ electrochemical sensor that had good response characteristics at pH 4−7.[26] However, a lot of environmental water samples are alkaline. Consequently, it is urgent to develop a HPO_4^{2-}-phosphate ion sensor with low cost, simple fabrication, and good stability for alkaline samples.

In current research, we will present a new type of all-solid phosphate-ion selective electrode. The tungsten pure metal was applied as the base electrode. First, we determined the modification potential of the reaction to form phosphotungstic acid ($H_3O_{40}PW_{12}{\cdot}xH_2O$) by cyclic voltammetry (CV). Then, the modified electrochemical method was applied at a three-electrode system. The tungsten electrode was electrodeposited under a constant potential certified by CV. Response characteristics to phosphate ions of the modified tungsten electrode were evaluated by potentiometry in a two-electrode system. The current phosphate ion sensor exhibits good performance in alkaline solutions successfully. Moreover, the responding mechanism of this sensor was explained clearly by scanning electron microscopy (SEM), XRD, UV−vis, and CV.

2. RESULTS AND DISCUSSION

2.1. Electrochemical Characteristics of Tungsten in Na_2HPO_4 Solution. In order to determine the reaction potential of the tungsten electrode with phosphate ions, the CV curve was analyzed. As shown in Figure 1, the tungsten electrode has an anode peak at about 0.6 V in sodium chloride at pH 9 and two obvious anodic peaks at 0.2 and 0.6 V in hydrogen phosphate disodium solution at pH 9. By comparing the two curves, it is preliminarily proved that the two peaks at 0.2 and 0.6 V may be related to the reaction of phosphate ions. In order to further explore the properties of these two anodic peaks, we tested the concentration dependence of the tungsten electrode in different phosphate solutions. As shown in Figure 2a, as the concentration of hydrogen phosphate disodium increases from 0.02 to 0.10 M, the positive peak of CV also rises. As for Figure 2b, we can clearly observe a good linear relationship between the concentration of hydrogen phosphate disodium and the peak current at 0.2 V of the corresponding cyclic voltammograms, with an *R*-square of 0.9982. It can be seen that the anodic peak is indeed from the reaction between the tungsten electrode and phosphate ions.

As phosphoric acid belongs to polybasic acids, it has three-stage dissociation in aqueous solutions. According to formula 1, it can be seen that the distribution proportion of phosphate ions in different dissociation states is also different under

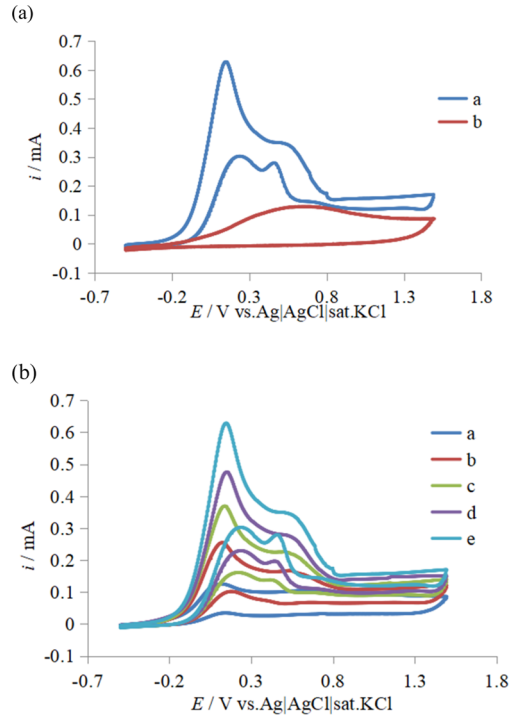

Figure 1. Cyclic voltammogram of the tungsten metal electrode in Na_2HPO_4 (a) and NaCl (b) at pH 9.

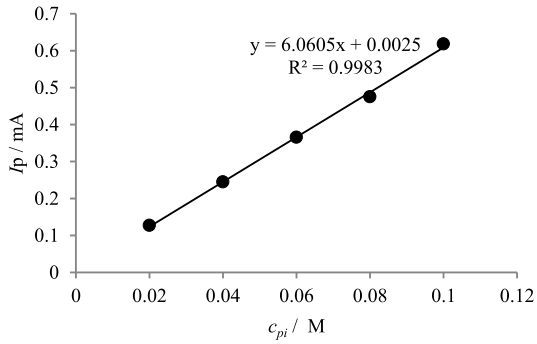

Figure 2. (a) Cyclic voltammograms in various concentrations of Na_2HPO_4 at pH 9.0: (a) 0.02, (b) 0.04, (c) 0.06, (d) 0.08, and (e) 0.10 M. (b) Concentration dependence of the cathodic peak current (I_p) at 0.2 V.

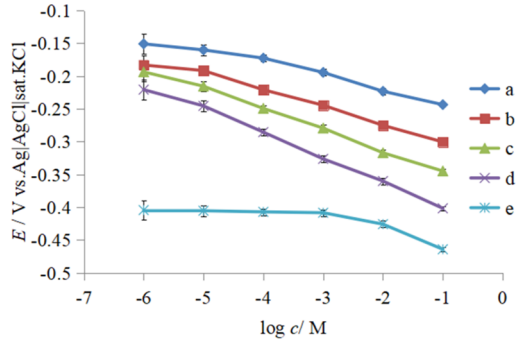

Figure 3. Influence of pH on the potential response of the modified tungsten electrode: (a) pH 7.0, (b) pH 8.0, (c) pH 9.0, (d) pH 10.0, and (e) pH 11.0.

different pH. Therefore, in order to identify which form of phosphate ion reacts with the tungsten electrode, we also

https://doi.org/10.1021/acsomega.1c00195
ACS Omega 2021, 6, 13795−13801

Table 1. Response Characteristics of References and Current Research

sensing type	sensing element/structure	detection range (M)	pH range	refs.
potentiometric	nano-IIP/CP	10^{-5} to 10^{-1}	acidic range	27
potentiometric	PTFE-Ag_3PO_4–Ag_2S	10^{-5} to 10^{-1}	5–8	28
potentiometric	CuMAPc-PnBA-coated Au electrode	4×10^{-9} to 10^{-2}	6–9	29
potentiometric	Mo electrode	10^{-5} to 10^{-1}	6.93–8.73	30
impedimetric	MWCNT/Ge/RTIL/CAA	10^{-6} to 10^{-1}	8.0–9.5	19
potentiometric	modified W	10^{-6} to 10^{-1}	7–10	current research

Table 2. Selectivity Coefficient of Common Anions Measured by the Mixed Solution Method

anion	log K_{pot}
NO_3^-	−2.8 ± 0.3
Cl^-	−4.2 ± 0.3
SO_4^{2-}	−4.5 ± 0.3
HCO_3^-	−2.8 ± 0.2
Ac^-	−3.0 ± 0.2

Table 3. Real-Sample Test Compared to Conventional Phosphomolybdate Blue Spectrometry

sample	W-ISE(mM)	colorimetry (mM)
Coca Cola	2.2 ± 0.2	2.4 ± 0.1
orange juice	4.0 ± 0.2	4.3 ± 0.1
wastewater	1.0 ± 0.2	1.1 ± 0.2

Table 4. Recovery Test in Different Solutions

sample	added (mM)	found (mM)	recovery rate (%)
distilled water	10.0	9.8 ± 0.1	98
tap water	10.0	9.8 ± 0.2	98
milk	10.0	9.5 ± 0.3	95

tested the CV curve of hydrogen phosphate disodium solution with different pH at the same concentration. It can be seen in Figure S1a that the anodic peak of the CV curve increases with the increase of pH value of hydrogen phosphate disodium solution

$$H_2PO_4^- + H_2O \rightleftharpoons HPO_4^{2-} + H_3O^+ \quad (1)$$

$$K_{a2} = \frac{[HPO_4^{2-}][H_3O^+]}{[H_2PO_4^-]} = 6.23 \times 10^{-8} \quad (2)$$

According to formula 1, the effective concentration of hydrogen phosphate at different pH was calculated, and it is found that the effective concentration is linear with the corresponding peak current (Figure S1b). Therefore, we can infer that the reaction with the tungsten electrode is hydrogen phosphate. In addition, we also explored the kinetic properties of the reaction (Figure S2). By analyzing the CV curves of different scanning rates, it was found that the peak currents were linearly related to the arithmetic square root of the scanning rate. It is concluded that the reaction is diffusion-controlled.

2.2. Modification of the Tungsten Electrode. Through a series of CV tests, we have a clear understanding of the basic properties of the electrochemical reaction between the tungsten electrode and phosphate ions. Based on this, we determined that the constant potential electrochemical modification potential is 0.2 V, and the electrolyte is 0.1 M hydrogen phosphate disodium at pH 9. The three-electrode

(a)

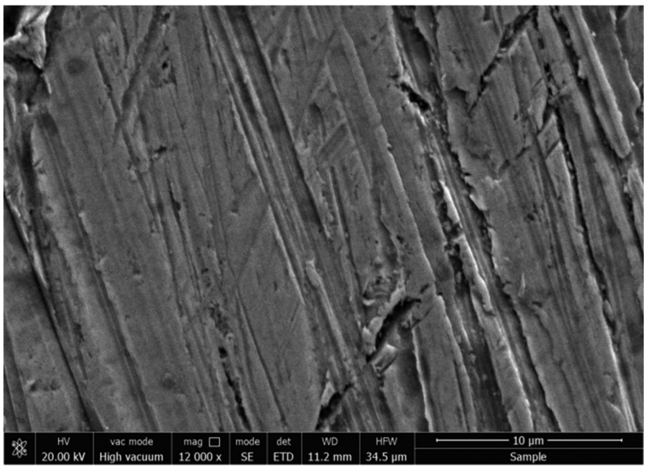

(b)

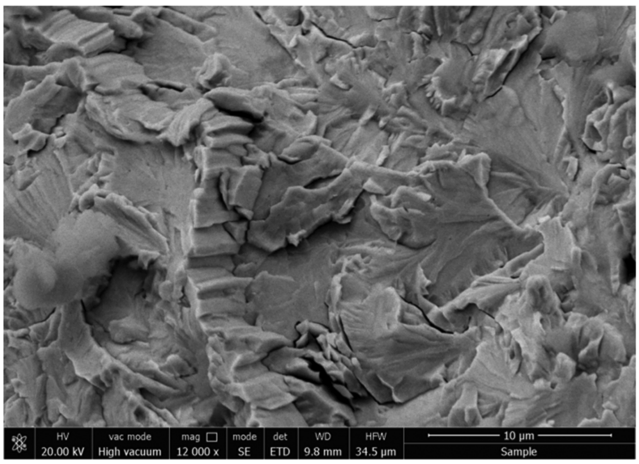

Figure 4. SEM of the tungsten electrode (a) and the modified tungsten electrode (b).

system was used for electrochemical modification. The tungsten electrode was used as the working electrode, Ag| AgCl was used as the reference electrode, and Pt was used as the counter electrode. In the process of constant potential electroplating, the metallic luster on the surface of the tungsten electrode gradually disappeared, and the color of the electrolyte changed from colorless transparent to light-yellow transparent. After 2 h of electroplating, the electroplating was stopped after the surface morphology of the electrode was no longer changed. At last, the modified electrode was dried for the test.

2.3. Response Characteristics of the Modified Tungsten Electrode. A series of tests on the response of the prepared tungsten modified electrode to phosphate ions

https://doi.org/10.1021/acsomega.1c00195
ACS Omega 2021, 6, 13795−13801

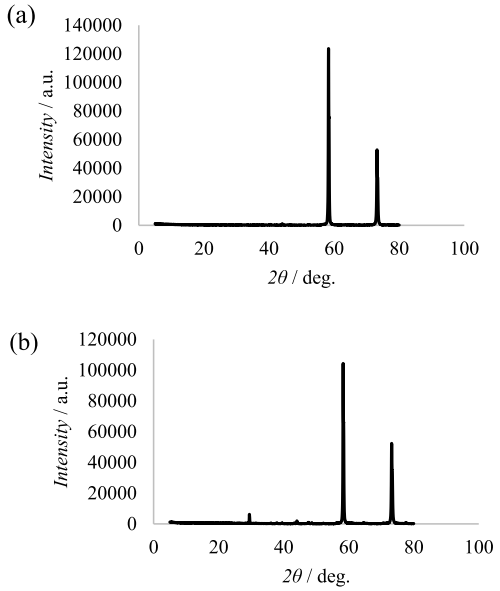

Figure 5. XRD patterns of (a) tungsten pure metal and (b) modified tungsten.

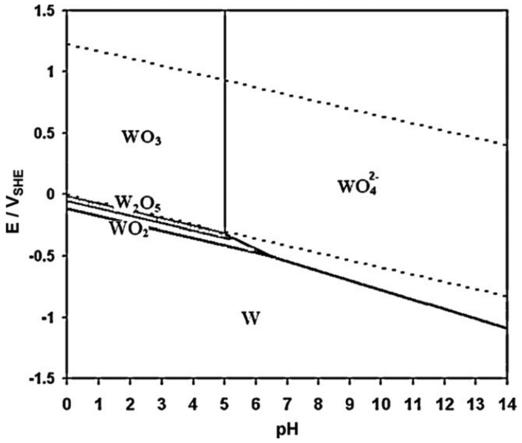

Figure 6. pH potential diagram of the W−H_2O system.[31]

were carried out using a two-electrode system. The tungsten modified electrode was used as the working electrode, and AgI AgCl was used as the reference electrode. We tested the phosphate standard solutions with different pH values. The phosphate standard solutions with different pH values were adjusted by using different concentrations of hydrochloric acid and sodium hydroxide based on dihydrogen phosphate sodium and hydrogen phosphate disodium. Therefore, the standard solution does not contain any other buffer solution. As shown in Figure 3, the detection limit of the sensor is about 10^{-5} M in the standard solution of pH 7 and pH 8 and about 10^{-6} M in the standard solution of pH 9 and pH 10, while in the standard solution of pH 11, the detection limit was less than 10^{-3} M due to the interference of OH^-. Therefore, the sensor can be applied to the detection of samples with pH from neutral to weak alkaline. The response slopes from pH 7 to pH 10 were −19.3, −24.6, −31.2, and −36.9 mV dec^{-1}, respectively. After removing the interference of OH^-, the corresponding slope is a near-Nernstian response.

As shown in Table 1, the current phosphate ion sensor possesses a relatively wide pH range for detecting phosphate ions compared to other reports. The response time was less

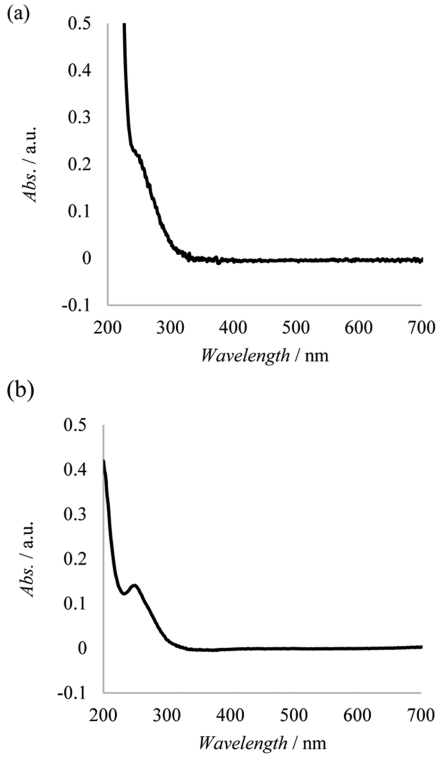

Figure 7. UV−Vis spectrometry of (a) electrolyte and (b) phosphotungstic acid.

than 1 min, and the potential fluctuation was less than ±3 mV within 24 h (Figure S3). After testing the disposable energy every week, it is found that the response curve of the sensor has no obvious change within 4 weeks. In Figure S4, the phosphate ion response characteristics of the modified tungsten electrode and the unmodified tungsten electrode were compared. The modified tungsten electrode showed a good reproducibility. As for the unmodified tungsten electrode, an obvious positive potential shift was observed due to the component change of the electrode surface. In the aspect of selectivity, we compared the interference of several common anions to the sensor by the mixed solution method based on formula 3

$$E_{ISE} = E' + \frac{RT}{n_B F}\ln(a_B + K^{pot}_{B,A} a_A^{n_B/n_A}) \quad (3)$$

The results in Table 2 show that the selectivity coefficients of all common anions were below −2, that is, there was no obvious interference on the detection of phosphate ions by the sensor. In addition, we also compared the sensor with the traditional spectral method and found that the detection results of the sensor are close to the traditional spectral method (Table 3).

In the addition recovery test, we considered that 10 mM phosphate ion was added to several common liquid samples, and the results showed that the recovery rate of all samples was above 95% (Table 4).This shows that the sensor can be used for the detection of phosphate ions in actual samples.

2.4. SEM Analysis of the Modified Tungsten Electrode. After evaluating the response performance of the sensor for phosphate ions, we analyzed its response mechanism. The surface morphology of the tungsten electrode was observed using a scanning electron microscope. On the surface of the

https://doi.org/10.1021/acsomega.1c00195
ACS Omega 2021, 6, 13795−13801

Scheme 1. Technical Routine of Modification and Evaluation of the Tungsten-Based Phosphate Ion Sensor

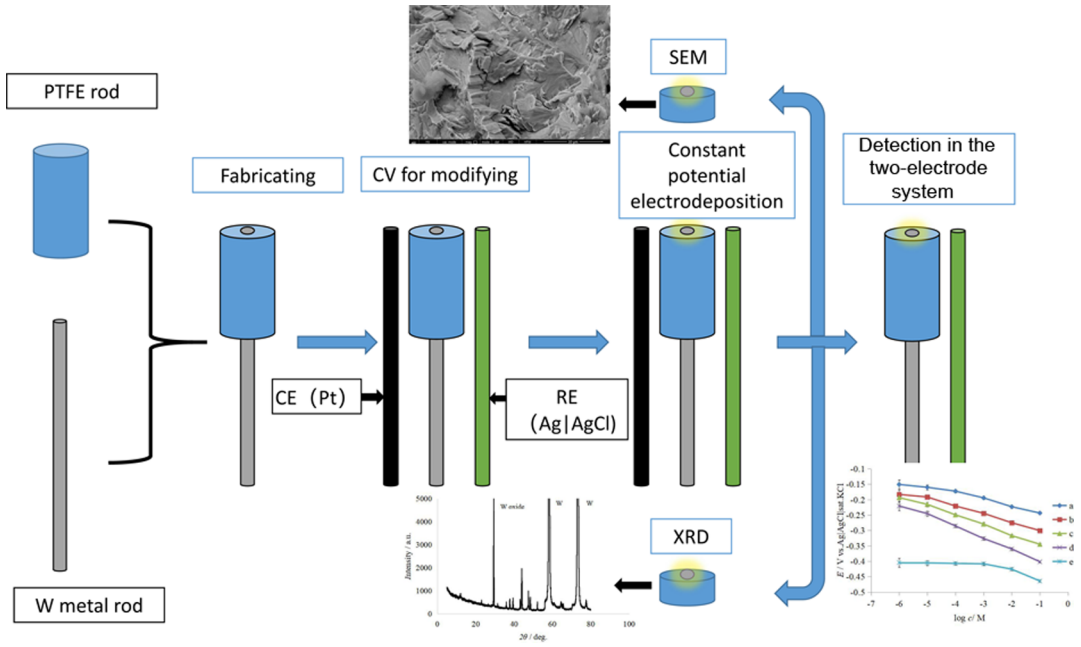

modified tungsten electrode, many electrolytic products with different shapes can be seen (Figure 4b).

2.5. XRD Analysis of the Modified Tungsten Electrode. In order to further explore the properties of the compounds attached on the surface of the modified tungsten electrode, we tried to identify the components of the surface attachment by X-ray diffraction (XRD). In order to facilitate the detection, we use 0.1 mm × 50 mm × 50 mm thin tungsten sheets in the XRD test, and the modification method is completely consistent with the above.

As shown in Figure 5a, there are two obvious peaks at 58° and 75° in the XRD spectrum of the pure metal tungsten sheet, which are the characteristic peaks of tungsten through database comparison. In addition to the two peaks of 58° and 75°, respectively, another peak appeared at 30° in the modified tungsten sheet. Through database comparison, the candidate compounds were all tungsten oxides of various forms. However, the specific results of tungsten oxide cannot be accurately determined by XRD. Therefore, we have consulted the relevant literature,[30] and combined with the pH potential diagram (Figure 6) of tungsten and the previous CV curve, we can preliminarily judge that the oxide is tungsten trioxide (WO_3).

2.6. UV−Vis Spectroscopy Analysis of the Solution after Electrodeposition. In order to further verify this judgment, we analyzed the composition of the Na_2HPO_4 electrolyte which turned pale yellow after electrochemical modification. The electrolyzed electrolyte was diluted 10 times and detected by UV−Vis spectroscopy (Figure 7a) and then compared with the standard sample solution of phosphotungstic acid (Figure 7b). The results showed that the spectral characteristics of the electrolyte and phosphotungstic acid were highly similar, and the absorption peaks appeared at about 250 nm.

It can be inferred that the main component of the electrolytic product is phosphotungstic acid. Through the above series of tests, we have analyzed the phosphate response mechanism of the sensor in detail. Based on the pH potential diagram, we can infer the surface component to tungsten oxide theoretically. According to XRD test, we can prove that the oxide was WO_3 in reality. Furthermore, we applied UV-Vis on the electrolyte solution, and the result shows that the composition of the solution was the same as $H_3O_{40}PW_{12}\cdot xH_2O$. Therefore, we can confirm that the response mechanism was as formula 4

$$2WO_4^{2-} + HPO_4^{2-} + 23H^+ \rightarrow PW_{12}O_{40}^{3-} + 12H_2O \quad (4)$$

3. CONCLUSIONS

We developed and designed a novel all-solid-state phosphate ion sensor based on the property that tungsten oxide can form a complex with phosphate ions. It is the first time to fabricate a phosphate ion sensor by the tungsten metal. This sensor possesses advantages of simple manufacture, low cost, a wide pH range for detecting, and good selectivity. The sensor is based on tungsten and electroplated at 0.2 V with sodium hydrogen phosphate at pH 9 as the electrolyte by constant potential electrolysis. A series of performance tests show that the sensor can produce Nernstian response to phosphate ions in the weak alkaline solution between pH 7 and pH 10. The linear range is 10^{-6} M to 0.1 M, the response time is less than 1 min, the error fluctuation of the 24 h continuous test is less than ±3 mV, the detection limit has no obvious change within 4 weeks, and it has good selectivity for common anions. The response mechanism was also elucidated by CV, XRD, SEM, and UV−Vis.

4. MATERIALS AND METHODS

4.1. Materials and Reagents. All chemicals were of analytical grade and used as received without further purification. All solutions were prepared with ultrapure water with a resistivity of 18.2 MΩ cm. Hydrogen phosphate disodium (Na_2HPO_4), sodium bicarbonate ($NaHCO_3$), sodium acetate (NaCOOH), sodium chloride (NaCl), sodium sulfate (Na_2SO_4), phosphotungstic acid ($H_3O_{40}PW_{12}\cdot xH_2O$),

https://doi.org/10.1021/acsomega.1c00195
ACS Omega 2021, 6, 13795−13801

hydrochloric acid (HCl), and sodium hydroxide (NaOH) were purchased from Xinke, Shenyang, China. Tungsten rods (φ2 mm × 100 mm, 99.99%) and tungsten plates (0.1 mm × 50 mm × 50 mm) were obtained from Guantai metal, Tianjin, China.

4.2. Apparatus. SEM was performed with a Quanta250-FEG field emission scanning electron microscope (FEI, Czech) accompanied by energy-dispersive spectrometry. XRD was performed with a D8 ADVANCE X-ray diffractometer system (BRUKER AXS GMBH, Germany). UV−Vis spectrometry was performed with a Lambda 650S (PerkinElmer, UK). Electrochemical measurements were carried out using a Versastat3 electrochemical workstation (Ametek, USA).

4.3. Preparation of the Tungsten Electrode. At first, the surface of the tungsten wire (diameter: 2 mm, length: 100 mm) was polished by sandpapers of #80, #240, and #1000, respectively. It was then washed for 30 min using an ultrasonic cleaner. One end of the tungsten wire was covered with a poly tetrafluoroethylene (PTFE, φ10 mm × 20 mm) tube at one end as a working electrode. The technical routine is shown as Scheme 1.

4.4. Cyclic Voltammogram Measurement. All measurements were carried out with a three-electrode system using a saturated AglAgCl reference electrode as a reference electrode, a tungsten electrode as a working electrode, and a platinum electrode as a counter electrode.

4.5. Modification of the Tungsten Electrode. Modification was applied with a three-electrode system. A saturated AglAgCl reference electrode was used as a reference electrode, a tungsten electrode was used as a working electrode, and a platinum electrode was used as a counter electrode. Constant potential electrodeposition was undertaken at 0.2 V in the solution of 0.1 M Na_2HPO_4 at pH 9 for about 2 h. After that, the modified tungsten electrode was dried by air to be tested.

4.6. Response Characteristics. All measurements were carried out with a two-electrode system using a saturated Agl AgCl reference electrode as a reference electrode and a tungsten electrode as a working electrode.

■ ASSOCIATED CONTENT

Supporting Information

The Supporting Information is available free of charge at https://pubs.acs.org/doi/10.1021/acsomega.1c00195.

Cyclic voltammograms in the presence of 0.1 M Na_2HPO_4 at various pH values; HPO_4^{2-} concentration dependence of the cathodic peak current (I_p) at 0.2 V; cyclic voltammograms in the presence of 0.1 M Na_2HPO_4 at pH 9.0 at various scanning rates; HPO_4^{2-} concentration dependence of the cathodic peak current (I_p) at 0.2 V; stability of the modified tungsten electrode for 24 h; phosphate ion response characteristics of the modified tungsten electrode and unmodified tungsten electrode at pH 9; and XRD patterns of the tungsten pure metal, modified tungsten, local enlarged image of the tungsten pure metal, and local enlarged image of modified tungsten (PDF)

■ AUTHOR INFORMATION

Corresponding Author

Ying Li − *School of Metallurgy, Northeastern University, Shenyang 110819, People's Republic of China; Liaoning Key Laboratory for Metallurgical Sensor Material and Technology, Shenyang 110819, People's Republic of China*; Email: liying@smm.neu.edu.cn

Authors

Kebin Xu − *School of Metallurgy, Northeastern University, Shenyang 110819, People's Republic of China; Liaoning Key Laboratory for Metallurgical Sensor Material and Technology, Shenyang 110819, People's Republic of China*; orcid.org/0000-0001-9378-0939

Min Li − *School of Metallurgy, Northeastern University, Shenyang 110819, People's Republic of China; Liaoning Key Laboratory for Metallurgical Sensor Material and Technology, Shenyang 110819, People's Republic of China*

Complete contact information is available at: https://pubs.acs.org/10.1021/acsomega.1c00195

Notes

The authors declare no competing financial interest.

■ ACKNOWLEDGMENTS

This work was financially supported by the National Natural Science Foundation of China (Project nos. 51774076, 51834004, 51904068, and 51474057) and the Fundamental Research Funds for the Central Universities (Project nos. N2125020).

■ REFERENCES

(1) Haberer, J. L.; Brandes, J. A. A High Sensitivity, Low Volume HPLC Method to Determine Soluble Reactive Phosphate in Freshwater and Saltwater. *Mar. Chem.* **2003**, *82*, 185−196.

(2) Diniz, M. C. T.; Filho, O. F.; de Aquino, E. V.; Rohwedder, J. J. R. Determination of phosphate in natural water employing a monosegmented flow system with simultaneous multiple injection. *Talanta* **2004**, *62*, 469−475.

(3) Björkman, K.; Thomson-Bulldis, A.; Karl, D. Phosphorus Dynamics in the North Pacific Subtropical Gyre. *Aquat. Microb. Ecol.* **2000**, *22*, 185−198.

(4) Protor, C. M.; Hood, D. W. Determination of inorganic phosphate in sea water by a butanol extraction procedure. *J. Mar. Res.* **1954**, *13*, 122−132.

(5) Rabalais, N. N. Nitrogen in Aquatic Ecosystems. *Ambio* **2002**, *31*, 102−112.

(6) Igwe, P. U.; Chukwudi, C. C.; Ifenatuorah, F. C.; Fagbeja, I. F.; Okeke, C. A. A Review of Environmental Effects of Surface Water Pollution. *Int. J. Eng. Sci.* **2017**, *4*, 128−137.

(7) Zaveri, E. D.; Russ, J. D.; Desbureaux, S. G.; Damania, R.; Rodella, A. S.; Giovanna, R. *The Nitrogen Legacy. In The Long-Term Effects of Water Pollution on Human Capital*; Policy Research Working Paper Series 9143; The World Bank, 2020.

(8) Wu, J.; Sunda, W.; Boyle, E. Phosphate depletion in the Western North Atlantic Ocean. *Science* **2000**, *289*, 759−762.

(9) Manghat, P.; Sodi, R.; Swaminathan, R. Phosphate Homeostasis and Disorders. *Ann. Clin. Biochem.* **2014**, *51*, 631−656.

(10) Copland, M.; Komenda, P.; Weinhandl, E. D.; Mccullough, P. A.; Morfin, J. A. Intensive Hemodialysis, Mineral and Bone Disorder, and Phosphate Binder Use. *Am. J. Kidney Dis.* **2016**, *68*, S24−S32.

(11) Su-Young, J.; Jaeyeol, K.; Seohyun, P.; Hyun, J. J.; Yun, H. R.; Hyoungnae, K.; Kyung, K. Y.; Chang-Yun, Y.; Chang, T. I.; Kang, E. W. Phosphate Is a Potential Biomarker of Disease Severity and Predicts Adverse Outcomes in Acute Kidney Injury Patients Undergoing Continuous Renal Replacement Therapy. *PLoS One* **2018**, *13*, No. e0191290.

(12) Li, J.; Wang, L.; Han, M.; Xiong, Y.; Liao, R.; Li, Y.; Sun, S.; Maharjan, A.; Su, B. The Role of Phosphate-Containing Medications and Low Dietary Phosphorus-Protein Ratio in Reducing Intestinal

Phosphorus Load in Patients with Chronic Kidney Disease. *Nutr. Diabetes* **2019**, *9*, 14.
(13) De Marco, R.; Phan, C. Determination of Phosphate in Hydroponic Nutrient Solutions Using Flow Injection Potentiometry and a Cobalt-Wire Phosphate Ion-Selective Electrode. *Talanta* **2003**, *60*, 1215−1221.
(14) Murphy, J.; Riley, J. P. A Modified Single Solution Method for the Determination of Phosphate in Natural Waters. *Anal. Chim. Acta* **1962**, *27*, 31−36.
(15) Jia, X.; Chen, D.; Bin, L.; Lu, H.; Zhang, R.; Zheng, Y. Highly Selective and Sensitive Phosphate Anion Sensors Based on AlGaN/GaN High Electron Mobility Transistors Functionalized by Ion Imprinted Polymer. *Sci. Rep.* **2016**, *6*, 27728.
(16) Quintana, J. C.; Idrissi, L.; Palleschi, G.; Albertano, P.; Amine, A.; El Rhazi, M.; Moscone, D. Investigation of Amperometric Detection of Phosphate: Application in Seawater and Cyanobacterial Biofilm Samples. *Talanta* **2004**, *63*, 567−574.
(17) Talarico, D.; Cinti, S.; Arduini, F.; Amine, A.; Moscone, D. Phosphate Detection through a Cost-Effective Carbon Black Nanoparticle-Modified Screen-Printed Electrode Embedded in a Continuous Flow System. *Environ. Sci. Technol.* **2015**, *49*, 7934.
(18) Bhat, K. S.; Nakate, U. T.; Yoo, J.-Y.; Wang, Y.; Hahn, Y.-B. Nozzle-Jet-Printed Silver/Graphene Composite-Based Field-Effect Transistor Sensor for Phosphate Ion Detection. *ACS Omega* **2019**, *4*, 8373.
(19) Norouzi, P.; Ganjali, M. R.; Faridbod, F.; Shahtaheri, S. J.; Zamani, H. A. Electrochemical Anion Sensor for Monohydrogen Phosphate Based on Nano-Composite Carbon Paste. *Int. J. Electrochem. Sci.* **2012**, *7*, 2633.
(20) Zina, F.; Nooredeen, N. M.; Azzouzi, S. Novel Sensitive Impedimetric Microsensor for Phosphate Detection Based on a Novel Copper Phthalocyanine Derivative. *Anal. Lett.* **2017**, *51*, 371.
(21) Nag, A.; Alahi, M. E. E.; Feng, S.; Mukhopadhyay, S. C. IoT-Based Sensing System for Phosphate Detection Using Graphite/PDMS Sensors. *Sens. Actuators, A* **2019**, *286*, 43−50.
(22) Ganjali, M. R.; Mizani, F.; Emami, M.; Niasari, M. S.; Shamsipur, M.; Yousefi, M.; Javanbakht, M. Novel Liquid Membrane Electrode for Selective Determination of Monohydrogenphosphate. *Electroanalysis* **2003**, *15*, 139−144.
(23) Reza, G. M.; Parviz, N.; Nader, H.; Masoud, S. N. Anion Recognition: Fabrication of a Highly Selective and Sensitive HPO4(2-) PVC Sensor Based on a Oxo-Molybdenum Methyl-Salen. *J. Braz. Chem. Soc.* **2006**, *17*, 859−865.
(24) Ganjali, M. R.; Norouzi, P.; Ghomi, M.; Salavati-Niasari, M. Highly Selective and Sensitive Monohydrogen Phosphate Membrane Sensor Based on Molybdenum Acetylacetonate. *Anal. Chim. Acta* **2006**, *567*, 196−201.
(25) Kumar, A.; Mehtab, S.; Singh, U.; Aggarwal, V.; Singh, J. Tripodal Cadmium Complex and Macrocyclic Ligand Based Sensors for Phosphate Ion Determination in Environmental Samples. *Electroanalysis* **2010**, *20*, 1186−1193.
(26) Xu, K.; Kitazumi, Y.; Kano, K.; Shirai, O. Phosphate ion sensor using a cobalt phosphate coated cobalt electrode. *Electrochim. Acta* **2018**, *282*, 242−246.
(27) Alizadeh, T.; Atayi, K. Synthesis of hydrogen phosphate anion-imprinted polymer via emulsion polymerization and its use as the recognition element of graphene/graphite paste potentiometric electrode. *J. Mol. Recognit.* **2018**, *209*, 180−187.
(28) Bralić, M. Preparation of Phosphate Ion-Selective Membrane Based on Silver Salts Mixed with PTFE or Carbon Nanotubes. *Int. J. Electrochem. Sci.* **2018**, *13*, 1390−1399.
(29) Abbas, M. N.; Radwan, A. L. A.; Nooredeen, N. M.; El-Ghaffar, M. A. A. Selective Phosphate Sensing Using Copper Monoamino-Phthalocyanine Functionalized Acrylate Polymer-Based Solid-State Electrode for FIA of Environmental Waters. *J. Solid State Electrochem.* **2016**, *20*, 1599−1612.
(30) Li, Y.; Jiang, T.; Yu, X.; Yang, H. Phosphate Sensor Using Molybdenum. *J. Electrochem. Soc.* **2016**, *163*, B479−B484.
(31) Anik, M. pH-dependent anodic reaction behavior of tungsten in acidic phosphate solutions. *Electrochim. Acta* **2009**, *54*, 3943−3951.

https://doi.org/10.1021/acsomega.1c00195
ACS Omega 2021, 6, 13795−13801